J Mater Sci (2008) 43:2745–2753
DOI 10.1007/s10853-008-2493-5

Sintering mechanism of fine zirconia powders with alumina added by powder mixing and chemical processes

Koji Matsui · Takanori Yamakawa · Masato Uehara · Naoya Enomoto · Junichi Hojo

Received: 6 June 2007 / Accepted: 24 January 2008 / Published online: 27 February 2008

Abstract The present study examined the sintering behavior of fine zirconia powders (containing 2.9 mol% Y_2O_3) with and without small amounts of Al_2O_3 added by different ways: powder mixing (PM), homogeneous precipitation (HP), and hydrolysis of alkoxide (HA). The initial sintering behavior was examined by both measurement methods of a constant rate of heating and isothermal shrinkage. In the PM process, Al_2O_3 particles pinned the shrinkage of zirconia powder compact at the initial stage and diffuse toward zirconia surface to enhance the sintering. This initial sintering mechanism was explained by the grain-boundary diffusion for the Al_2O_3-free powder and the volume diffusion for Al_2O_3-added powder. When Al_2O_3 was added to zirconia powder by HP and HA processes, the densification rate was more stimulated compared to the PM process. The initial sintering mechanism did not change by the way for Al_2O_3 addition. The Al_2O_3 addition by chemical processes of HP and HA tended to enhance the grain growth of zirconia, while the uniform microstructure was achieved because of homogeneous addition of Al_2O_3 by those processes.

Introduction

Yttria-stabilized tetragonal zirconia polycrystal (Y-TZP) has proved to be an important structural ceramic, with excellent mechanical properties, such as high fracture toughness, strength, and hardness, and has been commercialized for products of the optical fiber connector, grinding media, and precision parts. The appearance in Y-TZP with the higher mechanical properties and reliability is desired to spread the zirconia product market and to propel a new application development. The hydrolysis process is known as the industrial manufacturing one for Y-TZP powder. To develop a new Y-TZP powder with high quality that is excellent in forming and sintering characteristics by the hydrolysis process, it is important to analyze the sintering mechanism in Y-TZP powder produced by that and to clarify the sintering-control factors.

So far, the initial sintering on various ceramic powders has been investigated by many researchers [1–13]. Young and Cutler [1] quantitatively analyzed densification at the initial sintering stage measured under constant rates of heating (CRH) and have reported that the initial sintering stage of yttria-stabilized zirconia is explained by a mechanism of grain-boundary diffusion (GBD). Wang and Raj [2, 3] have estimated the activation energies at the intermediate sintering stage of zirconia (with Y_2O_3), and Al_2O_3/zirconia (with Y_2O_3) composite by the CRH method. In previous papers, the authors have studied kinetically the initial sintering behavior in Y-TZP powders with and without a small amount of Al_2O_3, and reported that a small amount of Al_2O_3 changes the diffusion mechanism from GBD to volume diffusions (VD) at the initial sintering stage and enhances the densification rate because of a decrease in the activation energy with the GBD→VD change [4, 5]. Furthermore, it has been reported that when the specific surface area of Y-TZP powder increases, the densification rate is enhanced because of an increase in the frequency factor at the initial sintering stage [6].

K. Matsui (✉)
Tokyo Research Laboratory, Tosoh Corporation, Ayase, Kanagawa 252-1123, Japan
e-mail: k_matui@tosoh.co.jp

T. Yamakawa · M. Uehara · N. Enomoto · J. Hojo
Department of Applied Chemistry, Kyushu University, Fukuoka 819-0395, Japan

Thus, the Al_2O_3 addition is a useful method to the sintering acceleration of Y-TZP powder. As also described in above reports [2–4], various Al_2O_3 powders are usually used as a starting raw material of additive to Y-TZP powder. From the standpoint of a new product development for Y-TZP powder, it is important to clarify the change of the sintering behavior that occurs by the difference in the process of Al_2O_3 addition. In particular, homogeneity of Al_2O_3 added to Y-TZP powder directly relates to the sintering rate and microstructure development. It is thought that homogeneity of Al_2O_3 added by chemical reaction rather than powder-addition processes is higher, but such an investigation that is noted to the Al_2O_3-addition process has not been reported in the previous papers.

The present study examined the sintering behavior of fine zirconia powders with and without small amounts of Al_2O_3 added by three different ways of powder mixing (PM), homogeneous precipitation (HP), and hydrolysis of alkoxide (HA).

Experimental procedure

Powder preparation

PM process

Fine zirconia powder containing 2.9 mol% (5.2 mass%) Y_2O_3 with a 15-m^2/g specific surface area (TZ-3Y grade, Tosoh, Tokyo, Japan) and fine Al_2O_3 powder (Alu C grade, Nippon Aerosil, Tokyo, Japan) with an $\sim$100-m^2/g specific surface area were used as starting raw materials. Two fine zirconia powders with 0.5 and 1 mass% Al_2O_3 addition were prepared by wet milling the fine zirconia and Al_2O_3 powders with a vibration mill. Here, distilled water was used as a dispersant. These prepared powders are named PM05A and PM10A, respectively. To compare with the sintering behavior of the powder with Al_2O_3 addition, the fine zirconia powder without Al_2O_3 addition (PM00A) also was prepared by wet milling only the fine zirconia powder under the same process.

HP process

The above fine zirconia powder (TZ-3Y grade) (5 g) was added to distilled water (100 cm^3), which was dispersed using an ultrasonic cleaner. $Al(NO_3)_3{\cdot}9H_2O$ (0.15 g) and $(NH_2)_2CO$ (3 g) (reagent, Wako Pure Chemical Industries, Osaka, Japan) were added to distilled water (100 cm^3). The slurry including zirconia, the mixed solution of $Al(NO_3)_3$ and $(NH_2)_2CO$, and a small amount of HNO_3 aqueous solution were mixed and then fully stirred. Here, HNO_3 was added in order to prepare stable solution. The pH of the resulting slurry was about 3. Next, this slurry was heated at 70 °C for 3 h while stirring. At this heating stage, as shown in Eqs. 1 and 2, OH^- ions were generated by the hydrolysis reaction of $(NH_2)_2CO$, the generated OH^- ions react with the Al^{3+} ions and aluminum hydroxide ($Al(OH)_3$) precipitates.

$$(NH_2)_2CO + 3H_2O \rightarrow 2NH_4^+ + CO_2 + 2OH^- \quad (1)$$

$$Al^{3+} + 3OH^- \rightarrow Al(OH)_3 \quad (2)$$

Using the centrifugation, the heat-treated slurry was filtrated and then washed with distilled water. The resulting powder was dried at 100 °C. Here, as shown in Eq. 3, amorphous $Al(OH)_3$ is dehydrated by drying and changes to amorphous hydrous alumina ($Al_2O_3{\cdot}(3\text{-}n)H_2O$).

$$2Al(OH)_3 \rightarrow Al_2O_3 \cdot (3\text{-}n)H_2O + nH_2O \quad (3)$$

Therefore, the resulting powder was a mixture of fine zirconia powder and hydrous alumina. The Al_2O_3 content in the powder by the chelate-titration method [14] was determined to be 0.39 mass%. This prepared powder is named HP04A.

HA process

To remove the moisture adsorbed on the particle surface, the above fine zirconia powder (TZ-3Y grade) was dried at 200 °C for overnight. The $(CH_3)_2CHOH$ (reagent, Wako Pure Chemical Industries) which was used as solvent was dehydrated using a molecular sieve. The dried powder (5 g) was added to the dehydration-treated $(CH_3)_2CHOH$ (100 cm^3) and then was dispersed using an ultrasonic cleaner. $Al(OCH(CH_3)_2)_3$ (reagent, Wako Pure Chemical Industries) (0.13 g) was dissolved in the $(CH_3)_2CHOH$ (100 cm^3). Both preparations of the dispersed slurry and the $Al(OCH(CH_3)_2)_3$ solution were conducted under N_2 atmosphere. NH_4OH solution with pH = 11 and $(CH_3)_2CHOH$ were mixed in the volume ratio 1:1. The dispersed slurry and the prepared $Al(OCH(CH_3)_2)_3$ solution were mixed, and the prepared NH_4OH solution (10 cm^3) was very slowly dropped into this mixed slurry while stirring. At this stage, as shown in Eq. 4, $Al(OH)_3$ is formed by the hydrolysis reaction of $Al(OCH(CH_3)_2)_3$.

$$Al(OCH(CH_3)_2)_3 + 3H_2O \rightarrow Al(OH)_3 + 3(CH_3)_2CHOH \quad (4)$$

Next, this resulting slurry was filtrated, washed, and dried by the same procedure as above. Therefore, this dried powder was also the mixture of fine zirconia powder and hydrous alumina. The Al_2O_3 content determined by the

same process as above was 0.66 mass%. This prepared powder is named HA07A.

CRH and isothermal shrinkage measurements

These powders were pressed uniaxially into a columnar disk under 60 MPa and afterward isostatically pressed at 300 MPa by rubber pressing. The size of the resulting powder compacts was about 5 mm∅ × 12 mm. The shrinkage of the powder compacts with sintering was measured by a thermomechanical analyzer (TMA; System TMA8310, Rigaku, Tokyo, Japan). In a TMA, the shrinkage proceeds isotropically because only a slight load was hung to the specimen during the measurement. The shrinkage measurements by CRH techniques were performed in the range from room temperature to 1,400 °C at a heating rate of 10 °C/min in air. When the temperature reached 1,400 °C, the specimens were cooled at a constant rate. Thermal expansions of the specimens were corrected from the observed shrinkages using the values corresponding to the thermal expansion coefficient that were determined from the slope of shrinkage-straight line observed in the cooling process. Assuming isotropic shrinkage to green compact, the density $\rho(T)$ at a given temperature T is given by the following Eq. 5 [2]:

$$\rho(T) = \left(\frac{L_f}{L(T)}\right)^3 \rho_f \tag{5}$$

where L_f and $L(T)$ are the final length and the length at a T of the specimen, respectively. ρ_f indicates the final density measured by the Archimedes method. The $\rho(T)$ value at a given temperature was calculated using Eq. 5. The isothermal shrinkage measurements were performed as follows: the temperature of the specimens was first increased at a constant rate of 10 °C/min to 600 °C, held at that temperature for 10 min, and subsequently increased rapidly at an about 50 °C/min rate to the set temperatures of 950 and 1,050 °C. The shrinkage was measured as a function of time at the constant set temperature for 19.7 h. When the time reached 19.7 h, the specimens were cooled at a constant rate. Thermal expansions of the specimens were corrected by the same method as above.

Preparation of sintered bodies and microstructure analysis

Prepared powders were pressed by the same process as above. Using the above TMA, the resulting green compacts were sintered at 1,200, 1,300, and 1,400 °C for 0 h at a heating rate of 10 °C/min in air. Scanning electron microscopy (SEM; Model S-5200, Hitachi, Tokyo, Japan) was used to measure the average grain sizes of the sintered bodies. Electron probe microanalyzer (EPMA; Model EMAX-5770W, Horiba, Tokyo, Japan) was used to identify Al_2O_3 grains existing in the sintered bodies. The specimens for both measurements were polished with a 3-μm diamond paste and then thermally etched for 0.5 h at a temperature lower by about 150–300 °C than the sintering temperature of each specimen in air. The average grain size was measured by the Planimetric method [15].

Results and discussion

PM process

Figure 1 shows changes of shrinkage in PM00A (without Al_2O_3), PM05A (with 0.5 mass% Al_2O_3), and PM10A (with 1 mass% Al_2O_3) in the course of heating at 10 °C/min. As can be seen in Fig. 1a, when the temperature passed ~1,100 °C, both shrinkages of PM05A and PM10A were remarkably greater than that of PM00A. Comparing the

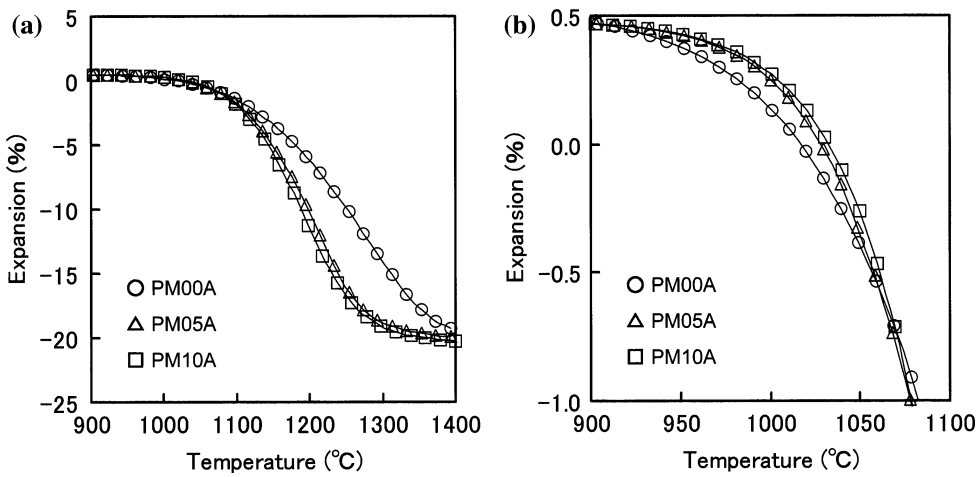

Fig. 1 Changes of shrinkage of PM00A, PM05A, and PM10A in the course of heating (10 °C/min)

shrinkage behavior PM05A with PM10A, the shrinkage of PM10A was slightly greater than that of PM05A. To exactly compare the initial shrinkage behavior of these specimens, the shrinkage curves were enlarged in the initial stage (Fig. 1b). The starting temperature of shrinkage was ~930 °C and nearly equal for PM00A, PM05A, and PM10A. Up to the temperature of 1,070 °C, the shrinkage of PM00A was greater than those of PM05A and PM10A, whereas beyond this temperature, shrinkages of both PM05A and PM10A increased rather than that of PM00A. This behavior agreed with that of fine zirconia powders with and without 0.23 mass% Al_2O_3 prepared by the PM process in the previous paper [4]. Using the shrinkage curves in Fig. 1a, the temperature dependences of the relative density were determined by Eq. 5 (Fig. 2). Here, the relative densities were calculated using the theoretical density (6.05 g/cm^3) of 3 mol% Y-TZP [16] because the amount of added Al_2O_3 was little. Beyond ~1,100 °C, both relative densities of PM05A and PM10A were apparently greater than that of PM00A, and the shrinkage of PM10A was slightly greater than that of PM05A. These results reveal that the densification–acceleration action is almost the same at Al_2O_3 concentrations of ≥0.5 mass%.

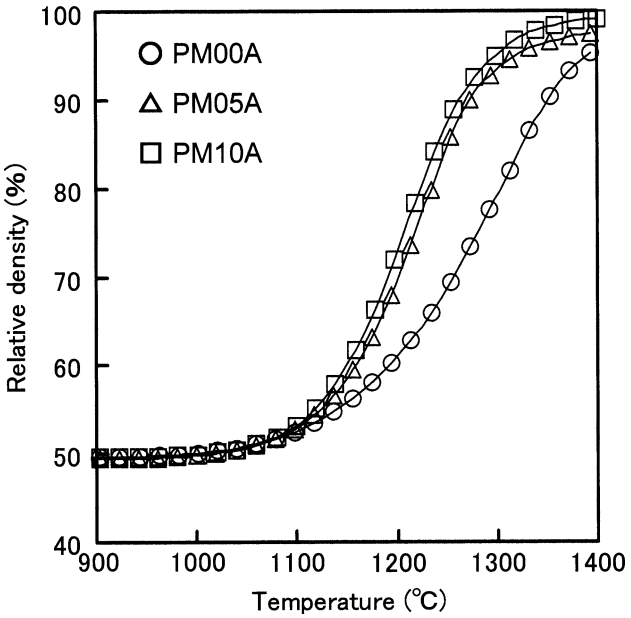

Fig. 2 Changes of relative density of PM00A, PM05A, and PM10A with temperature

Figure 3 shows changes of shrinkage with heating time of PM00A and PM10A measured at set temperatures of 950 and 1,050 °C. At 950 °C, up to first 8h, the shrinkage of PM00A was greater than that of PM10A, but after that time, the shrinkage of PM10A increased. At 1,050 °C, the shrinkage rate of PM10A was remarkably greater than that of PM00A. Taking into account both results in Figs. 1b and 3 (950 °C), it is concluded that Al_2O_3 particles pin the shrinkage of powder compact at the region where the shrinkage of PM00A was greater than that of PM05A or PM10A.

It is presumed that the densification–acceleration effect by Al_2O_3 addition occurs by the change of diffusion mechanism. The diffusion mechanism at the initial sintering stage was determined to clarify this presumption. The sintering-rate equation of isothermal shrinkage at the initial sintering stage is given by the following Eq. 6 [7]:

$$\left(\frac{\Delta L}{L_0}\right) = \left(\frac{K\gamma\Omega D}{kTa^p}\right)^n t^n \tag{6}$$

On taking logarithms, the following equation is obtained:

$$\log\left(\frac{\Delta L}{L_0}\right) = n\log\left(\frac{K\gamma\Omega D}{kTa^p}\right) + n\log t \tag{7}$$

where $\Delta L(= L_0 - L)$ is the change in length of the specimen, L_0 the initial length of the specimen, K the numerical constant, γ the surface energy, Ω the atomic volume, D the diffusion coefficient, t the time, T absolute temperature, k

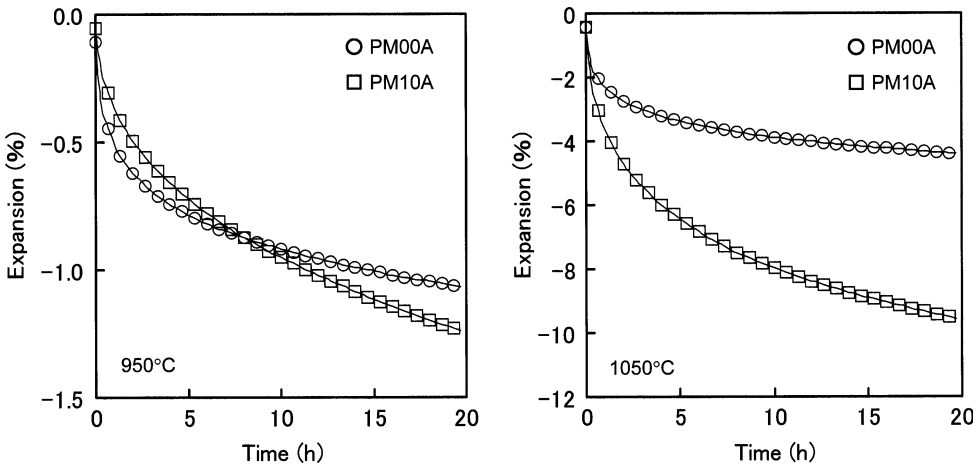

Fig. 3 Changes of shrinkage with heating time of PM00A and PM10A measured at set temperatures of 950 and 1,050 °C

the Boltzmann's constant, a the spherical particle radius, and the parameters n and p the order depending on the diffusion mechanism. The K includes the effective grain-boundary width in GBD [7]. The values of p for GBD and VD are $p = 4$ and $p = 3$, respectively. Eq. 6 is applicable to the fractional shrinkages of <4%, which satisfies the initial sintering condition. In a shrinkage range below 4%, the isothermal shrinkage curves in Fig. 3 were converted to log–log plots (Fig. 4), and the n values were determined from the slopes of the straight lines (Table 1). According to two-sphere shrinkage models proposed by several researchers, it has been reported that the n value ranges of GBD and VD were $n = 0.31$–0.33 and 0.40–0.50, respectively [7]. Comparing them with the n values determined experimentally in Table 1, it was confirmed that the diffusion mechanisms of PM00A and PM10A were GBD and VD, respectively. The isothermal shrinkage behavior of PM05A was also measured and analyzed by the same method, and the diffusion mechanism was assigned to VD (Table 1). Therefore, the densification–acceleration effect by Al_2O_3 powder addition can be explained by the GBD→VD change at the initial sintering stage.

Figure 5 shows SEM images of PM00A, PM05A, and PM10A sintered at 1,400 °C for 0 h. Grains which look blackish were observed in PM05A and PM10A, and it was confirmed that the blackish grains were Al_2O_3 from the result of EPMA measurements. This result suggests that a part of added Al_2O_3 powder is formed as the Al_2O_3 grain at the sintering process. To quantitatively examine the effect of Al_2O_3 on the grain-growth behavior, the average grain sizes of PM00A and PM10A sintered at 1,200–1,400 °C were determined by the Planimetric method (Fig. 6). The relative density of each specimen corresponded nearly to the result in Fig. 2. At 1,200 °C, the average grain size of PM10A was nearly equal to that of PM00A. At temperatures ≥1,300 °C, the average grain size of PM10A was slightly greater than that of PM00A. This result reveals that Al_2O_3 powder addition slightly accelerates the grain-growth process though Al_2O_3 grains are formed at the sintering process.

Table 1 Orders (n values) depending on the diffusion mechanism

Specimen	n value	
	950 °C	1,050 °C
MP00A	0.33	0.33
MP05A	0.43	0.42
MP10A	0.45	0.44
HP04A		0.46
HA07A		0.44

HP and HA processes

Figure 7a shows changes of shrinkage in HP04A (with 0.39 mass% Al_2O_3) and HA07A (with 0.66 mass% Al_2O_3) in the course of heating at 10 °C/min. The shrinkage curves that were enlarged in the initial stage are also shown in Fig. 7b. CRH data of PM00A and PM10A in Fig. 1 were also plotted in Fig. 7 to compare the shrinkage behavior of powder compacts prepared by PM with HP and HA processes. The shrinkage-starting temperature of both HP04A and HA07A was ∼930 °C and nearly equal to PM00A, PM05A, and PM10A. Above this shrinkage-starting temperature, both shrinkages of HP04A and HA07A were slightly greater than that of PM10A. The temperature dependences of the relative density were also determined using the shrinkage curves in Fig. 7a (Fig. 8). It was seen that the densifications of HP04A and HA07A were slightly accelerated as compared to that of MP10A. These results reveal that nevertheless Al_2O_3 contents of both HP04A and HA07 are less than that of PM10A; those densifications are accelerated more slightly than that of PM10A.

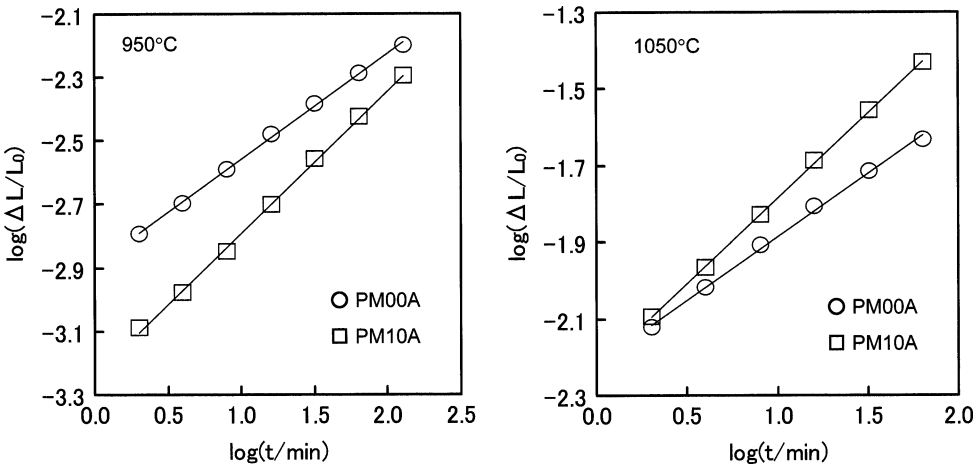

Fig. 4 Logarithm shrinkage–logarithm time plots of PM00A and PM10A measured at the set temperatures of 950 and 1,050 °C

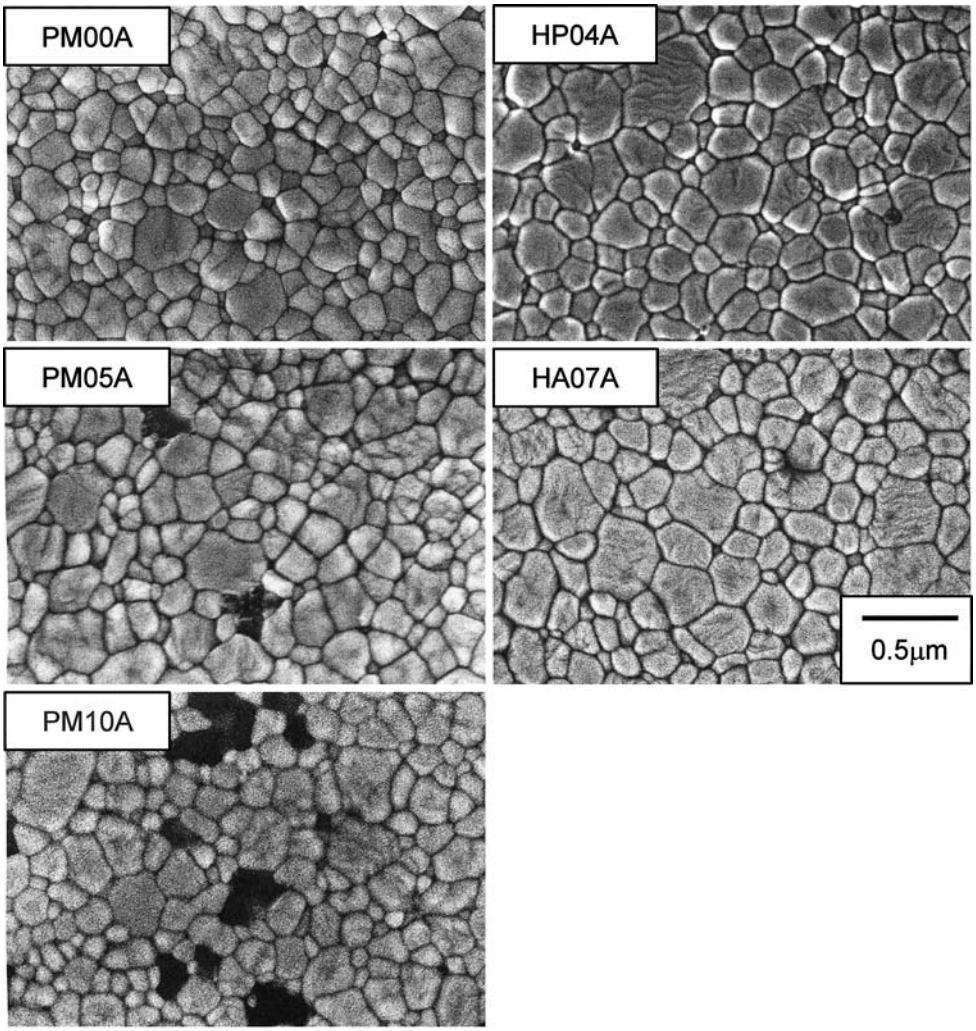

Fig. 5 Scanning electron microscopy images of PM00A, PM05A, PM10A, HP04A, and HA07A sintered at 1,400 °C

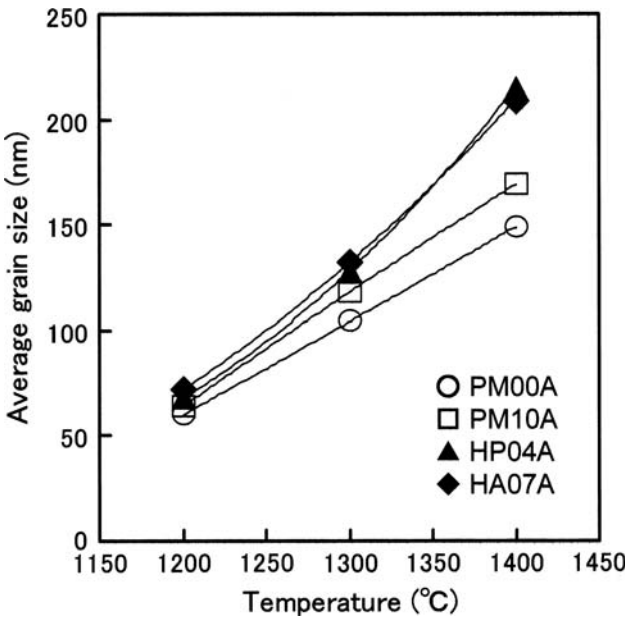

Fig. 6 Changes of average grain size in MP00A, MP10A, HP04A, and HA07A with sintering temperature

Figure 9a shows changes of shrinkage with heating time of HP04A and HA07A measured at the set temperature of 1,050 °C. Isothermal shrinkage data of PM00A and PM10A in Fig. 3 were also plotted in Fig. 9a. The shrinkage rates of HP04A and HA07A were slightly and clearly greater than that of MP10A, respectively, which is consistent with the results in Fig. 7. In a shrinkage range below 4%, the isothermal shrinkage curves were converted to the log–log plots (Fig. 9b), and the n values were determined from the slopes of the straight lines. As shown in Table 1, diffusion mechanisms of both HP04A and HA07A were assigned to VD that is the same diffusion mechanism as the PM process. Therefore, it was clarified that the sintering mechanism did not change by the way for Al_2O_3 addition.

SEM images of HP04A and HA07A sintered at 1,400 °C for 0 h are shown in Fig. 5. A blackish Al_2O_3 grain, which was observed in PM05A and PM10A could be scarcely confirmed in the sintered bodies. This result reveals that Al_2O_3, which was added by HP and HA rather

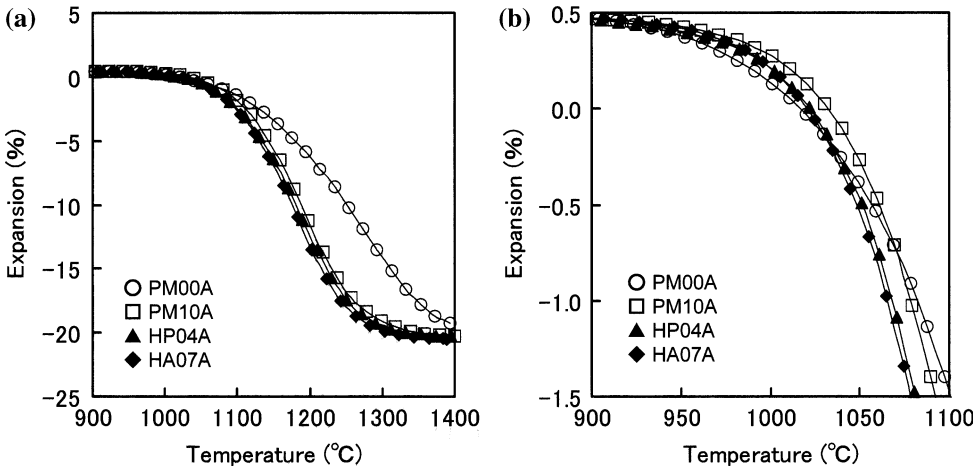

Fig. 7 Changes of shrinkage of PM00A, PM10A, HP04A, and HA07A in the course of heating (10 °C/min)

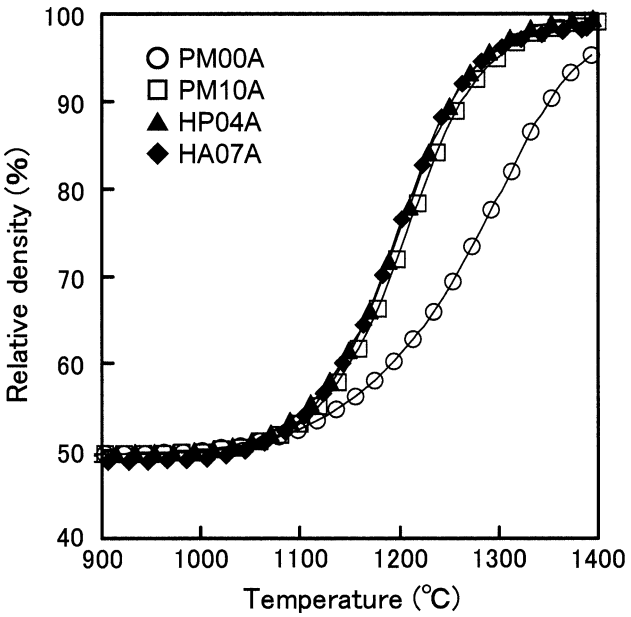

Fig. 8 Changes of relative density of PM00A, PM10A, HP04A, and HA07A with temperature

than PM processes, homogeneously exists in the sintered bodies. To quantitatively examine the influence by the difference in the Al_2O_3-addition process on the grain-growth behavior, the average grain sizes of HP04A and HA07A sintered at 1,200–1,400 °C were plotted in Fig. 6. The relative density of each specimen corresponded nearly to the result in Fig. 8. At 1,200 °C, the average grain sizes of HP04A and HA07A were nearly the same as those of PM00A and PM10A. At temperatures $\geq$1,300 °C, the average grain sizes of HP04A and HA07A were apparently greater than that of PM10A. This result reveals that the Al_2O_3 addition by the HP and HA processes tended to further enhance grain growth as compared with that by the PM process.

Effect of Al_2O_3-addition process on sintering mechanism

It is generally known for the comparison in the same oxide (without additive) that the activation energy of VD is higher than that of GBD. Therefore, for zirconia without Al_2O_3, the activation energy of VD is higher than that of

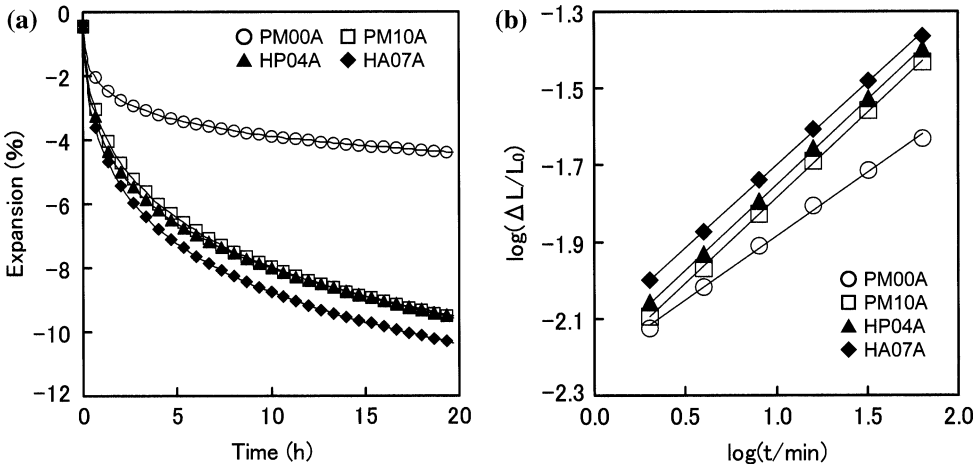

Fig. 9 Changes of shrinkage with heating time and logarithm shrinkage–logarithm time plots of PM00A, PM10A, HP04A, and HA07A measured at the set temperature of 1,050 °C

GBD, which means that GBD is the diffusion process at a low temperature region, whereas VD is the diffusion process at a high temperature region. In the present results, added Al_2O_3 changed the diffusion mechanism at the initial sintering stage from GBD to VD. Furthermore, in the previous paper, the authors reported that contrary to the general tendency above, the activation energy of VD in fine zirconia powder with 0.23 mass% Al_2O_3 added by the PM process was lower than that of GBD in fine zirconia powder without Al_2O_3 [4]. This evidently exhibits that added Al_2O_3 directly affects the diffusion mechanism at the initial sintering stage, and the action mechanism of added Al_2O_3 was discussed as follows [4]. In the temperature region where the shrinkage is not observed, added Al_2O_3 interferes with neck formation and growth by surface diffusion. However, when the temperature increases, a part of added A_2O_3 particles begins to dissolve in zirconia particles, dissolved Al_2O_3 changes the diffusion mechanism from GBD to VD, and the densification rate remarkably increases. In the results obtained for HP and HA processes, at the beginning region of shrinkage, shrinkages of both HP04A and HA07A were slightly less than that of PM00A, whereas beyond 1,030 °C, these shrinkages were remarkably greater than that of PM00A (Fig. 7b) and Al_2O_3 added by theses processes changed the diffusion mechanism from GBD to VD (Table 1). This behavior is also explained by the diffusion mechanism in the previous paper [4]. Thus, the effect of Al_2O_3 addition can be reasonably interpreted by assuming the segregated dissolution of Al_2O_3 on the zirconia surface, and the validity of this assumption has been demonstrated by the reports in Matsui et al. [17, 18]. In their analytical results, it was shown that no amorphous layer exists along the grain-boundary faces in its 0.25 mass% Al_2O_3-doped 2.9 mol% Y-TZP, but Y^{3+} and Al^{3+} ions segregate at grain boundaries over widths of $\sim$10 and $\sim$6 nm, respectively. Furthermore, at the sintering temperature of 1,100 °C, Al^{3+} ions segregated at grain boundaries, and the segregation of Al^{3+} ions increased with increasing sintering temperature [18].

Taking into account these reports, it is presumed that when homogeneity of Al_2O_3 on the zirconia surface becomes high (i.e., the number of the contacted points between Al_2O_3 and the zirconia surface increases), the densification rate increases because the densification-accelerated field (where Al_2O_3 dissolves and segregates) increases. The present results reveal that nevertheless Al_2O_3 contents of both HP04A and HA07 are less than that of PM10A,;those densifications are accelerated more slightly than that of PM10A. As shown in Fig. 5, in PM05A whose the Al_2O_3 content was roughly equal to those of HP04A and HA07A, Al_2O_3 grains which did not dissolve and segregate were observed, whereas an Al_2O_3 grain was scarcely confirmed in both HP04A and HA07A. Taking into account these results, it is concluded that Al_2O_3 added by both HP and HA processes homogeneously exists on the particle surface of zirconia as compared with finer Al_2O_3 particles added by the PM process. Therefore, the addition of Al_2O_3 to zirconia powder by HP and HA processes is effective to the stimulation of the densification compared to the PM process.

Matsui et al. have reported that the grain-growth mechanism in Y-TZP is reasonably interpreted by the solute-drag effect of Y^{3+} ions segregating along grain boundaries [19], and when a small amount of Al_2O_3 is doped to Y-TZP, Al^{3+} ions segregated at grain boundaries have the effect of enhancing grain-boundary diffusion [18]. Based on these results, they discussed that when the segregation of Al^{3+} ions increases with increasing sintering temperature, the predominant effect that enhances grain-boundary diffusion is caused by Al^{3+} ions rather than the solute-drag effect of Y^{3+} ions, and as a result, the grain-growth behavior of a small amount of Al_2O_3-doped Y-TZP is enhanced more rapidly than that of Y-TZP [18]. Okada and Sakuma [20] have reported the microstructure and grain-growth behavior in Al_2O_3-2.5 mol% Y-TZP composites with Y-TZP content of 3.3-93.3 vol%. They showed that in Al_2O_3-rich contents, the growth of coarse Al_2O_3 grains was effectively retarded by fine Y-TZP grains, whereas in Y-TZP-rich contents, the size of Al_2O_3 grains was almost the same as that of Y-TZP grains and they little influenced the growth of Y-TZP grains. It was explained that the grain-boundary pinning by minor phase grains is only effective when major phase grain-growth rate is sufficiently high, i.e., the results obtained for Y-TZP-rich contents were related to the sluggish grain growth in Y-TZP. According to the result in Fig. 6, at 1,200 °C, the average grain size of PM10A was nearly equal to that of PM00A though Al_2O_3 grains are formed at the sintering process. At temperatures $\geq$1,300 °C, the average grain size of PM10A became slightly greater than that of PM00A. This result apparently reveals that Al_2O_3 grains which are observed in Fig. 5 (PM05A and PM10A) little influence the grain growth as the grain-boundary pinning, which is explained by the above consideration reported by Okada and Sakuma.

The present results reveal that the Al_2O_3 addition accelerates the grain-growth process, and the Al_2O_3 addition by the HP and HA processes tends to further enhance grain growth as compared with that by the PM process (Fig. 6). Analogizing from the report in Matsui et al. [17], it is speculated that the segregations of Al^{3+} ions during sintering of HP04A and HA07A are greater than those of PM05A and PM10A, and as a result, grain growths of HP04A and HA07A are further enhanced. Taking into account that an Al_2O_3 grain was scarcely observed in PM05A and PM10A (Fig. 5), this speculation is

reasonable. On the other hand, Al_2O_3 and ZrO_2 (without Y_2O_3) are known to exhibit very limited mutual solubility [21, 22]. Therefore, most of Al_2O_3 added by the HP and HA processes segregate at the grain-boundary vicinities after sintering. Such a uniform microstructure in a small amount of Al_2O_3-doped Y-TZP was achieved because of homogeneous addition of Al_2O_3 by chemical processes of HP and HA.

Conclusions

The present study examined the sintering behavior of zirconia powders with and without small amounts of Al_2O_3 prepared by three different ways of PM, HP, and HA. The following conclusions were obtained:

(1) When Al_2O_3 was added to zirconia powder by HP and HA processes, the densification rate was more stimulated compared to the PM process. This result reveals that Al_2O_3 added by HP and HA processes homogeneously exists on the particle surface of zirconia as compared with finer Al_2O_3 particles added by the PM process.

(2) The diffusion mechanism at the initial sintering stage changed from GBD to VD by Al_2O_3 addition. The VD mechanism did not change by three different ways of PM, HP, and HA for Al_2O_3 addition.

(3) The Al_2O_3 addition by the chemical process tended to enhance the grain growth of zirconia. Such a uniform microstructure in a small amount of Al_2O_3-doped Y-TZP was achieved because of homogeneous addition of Al_2O_3 by the HP and HA processes.

References

1. Young WS, Cutler IB (1970) J Am Ceram Soc 53:659
2. Wang J, Raj R (1990) J Am Ceram Soc 73:1172
3. Wang J, Raj R (1991) J Am Ceram Soc 74:1959
4. Matsui K, Ohmichi N, Ohgai M, Yamakawa T, Uehara M, Enomoto N, Hojo J (2004) J Ceram Soc Jpn 112(5, Suppl. 112-1, PacRim5 Special Issue):S343
5. Matsui K, Ohmichi N, Ohgai M, Enomoto N, Hojo J (2005) J Am Ceram Soc 88:3346
6. Matsui K, Matsumoto A, Uehara M, Enomoto N, Hojo J (2007) J Am Ceram Soc 90:44
7. Johnson DL (1969) J Appl Phys 40:192
8. Johnson DL, Cutler IB (1963) J Am Ceram Soc 46:541
9. Johnson DL, Cutler IB (1963) J Am Ceram Soc 46:545
10. Moriyoshi Y, Komatsu W (1971) Yogyo Kyokai Shi 79:370
11. Moriyoshi Y, Komatsu W (1970) J Am Ceram Soc 53:671
12. Su H, Johnson DL (1996) J Am Ceram Soc 79:3211
13. Ikegami T (1998) J Ceram Soc Jpn 106:456
14. Ueno K (1989) In: Kireto Tekitei Hou (Chelate-titration method), Nankodo, Tokyo, Japan, pp 111–115 (in Japanese)
15. Yamaguchi T (1984) Ceramics Jpn 19:520
16. Abe H, Kanno T, Kawai M, Suzuki K (1984) In: Yamaguchi T, Yanagita H (eds) Enjiniaringu Seramikkusu (Engineering ceramics), Gihodo, Tokyo, Japan, pp 22–24 (in Japanese)
17. Matsui K, Horikoshi H, Ohmichi N, Ohgai M, Yoshida H, Ikuhara Y (2003) J Am Ceram Soc 86:1401
18. Matsui K, Ohmichi N, Ohgai M, Yoshida H, Ikuhara Y (2006) J Mater Res 21:2278
19. Matsui K, Ohmichi N, Ohgai M, Yoshida H, Ikuhara Y (2006) J Ceram Soc Jpn 114:230
20. Okada K, Sakuma T (1992) J Ceram Soc Jpn 100:382
21. Hodgson SNB, Cawley J, Clubley M (1999) J Mater Process Tech 92–93:85
22. Ondik HM, Mcmurdie HF (eds) (1998) Phase diagrams for zirconium and zirconia systems. Am Ceram Soc, Ohio, p 63